International Conference on Computational and Experimental Methods in Mechanical Engineering
G.L. Bajaj Institute of Technology and Management, Greater Noida (U.P) India ICCEMME-2017
8th- 9th December 2017, www.conferenceworld.in ISBN: 978-93-86171-85-6

CFD Analysis of Two-phase Flow Characteristics in Horizontal Pipeline

Navneet Kumar [1,*], Desh Bandhu Singh [1], Sanjeev Kumar Sharma[2]

[1]*Department of Mechanical Engineering, Galgotias College of Engineering & Technology, Greater Noida, G.B. Nagar, Uttar Pradesh – 201306, INDIA*

[2]*Department of Mechanical Engineering, Amity University, Noida, UTTAR PRADESH, INDIA*

ABSTRACT

This paper shows numerical simulation of horizontal slurry flow (water-glass beads) of finer particles through pipeline. Glass beads slurry in water having 125 µm mean diameter particles is analyzed through 54.9 mm diameter pipe at concentrations up to 50% flowing with varying flow velocities up to 5 m/s. 3-D Computational Fluid Dynamics (CFD) Eulerian model with RNG k-ε turbulence closure is adopted to analyze the mono-dispersed glass beads particles of density 2470 Kg/m3. The flow characteristics of slurries conveying through pipeline were simulated using FLUENT commercial software applying Eulerian two-phase flow model. Concentration and velocity profiles were predicted and analyzed vis-a-vis observed flow features to understand the transport mechanism of solid-liquid flow in slurry mode. Qualitative aspects of this analysis have also been presented in the paper.

Keywords: 3-D CFD Modelling, Concentration Distribution, Slurry Pipeline, Slip-Velocity.

1. INTRODUCTION

Conveying of granular solids in slurry form through pipeline systems is widely applied in industries due to its several inherent advantages, such as, continuous delivery, flexible routing, ease in automation and long distance transport capability, etc.The designing of slurry pipeline requires better understanding of concentration profiles, pressure drop and deposition velocity of solids. Many researches since the start of third decade of 20th century have tried to develop general solution for these parameters based on limited set of experimental data. The first few attempts in this area was made by O'Brien (1933) and Rouse (1937) in which they predicted the concentration distribution using diffusion model and applied it to open channel flows having very low volumetric solid concentration. Ismail (1952) further modified the simple diffusion model by correlating coefficient of mass transfer to shear velocity gradient.

In fact, the present knowledge base of slurry pipeline design is still not complete, particularly for higher concentration slurries, since the designers of slurry transport systems yet rely on the data generated from pilot plant test facility. Additionally, a huge cost involved in setting up a new slurry pipeline system demands for the

cost to be minimized. Advent of highly sophisticated computers with advanced numerical techniques involved in computational fluid dynamics (CFD) analysis made it possible to analyze the operation of slurry transport systems using numerical simulations. CFD gives detailed information about the local variations of flow parameters and allow a researcher to conduct parametric studies with greater ease and at extremely low cost; which otherwise is quite expensive, time consuming and laborious experiments to be performed on pilot plant test facility. Krampa-Morlu et. al. (2004) did numerical investigation of the flow parameters in a vertical pipeline having slurry flows of courser particles using *k-ε* turbulence model for each phase and investigated the effect of particle size, efflux concentration and solid viscosity on various flow parameters. Ling et. al. (2003) used algebraic slip mixture (ASM) model for numerical solution for sand-water slurry flow in a straight horizontal pipe for a range of mean solid concentrations which were found be in good agreement with experimental results for slurry mean velocity higher than deposition velocity. Lin and Ebadian (2007) numerically investigated sand-water slurry flows in the entrance region of horizontal pipe using ASM model and analyzed the development of various flow parameters in the entrance region of horizontal pipe.

Jiang and Zhang (2012) performed 2-D numerical simulations on slush nitrogen flow in horizontal pipe of 15 mm diameter and length of 1.5 m, and particle diameter is 1.0 mm by using per-phase *k-ε* turbulence model to model the turbulent two phase flow. They concluded that 2-D multiphase model has the advantage over the 3-D model due to the excessive computational time that the 3-D calculation incurs. Recently, Kumar et. al. (2016, 2017) performed CFD modeling for slurry flows of at higher concentrations and recommended Eulerian model as it predicts both pressure drop and solid concentration profiles quite accurately.

In this study, per-phase RNG *k-ε* turbulence model is used to model the turbulent two-phase flow, and the motion of solid phase is modeled by the kinetic theory of granular flow to account for both particle–particle and particle–wall interactions. The 3-D multiphase model is performed with our earlier experimental work by Kaushal et. al. (2005). The aim of this work is to check the capability of CFD to predict such complex slurry flow and thus facilitate their modeling for research and industrial design purposes.

II **MATHEMATICAL MODEL**

During numerical analysis of slurry pipeline flows, the selection of appropriate multiphase model depends mainly on the range of volume fraction (α) of solid phase under consideration. In present work, Eulerian model of granular version has been adopted as it is best suited for such flows especially when volume fractions of solid phase are higher. This is so because it captures the effect of friction and collusions between particles quite effectively which is quite dominating in higher concentration slurries having courses particles.

2.1 Eulerian Model

In Eulerian model, slurry is assumed to be consists of solid "s" and fluid "f" phases which are separating, yet maintain interpenetrating continua such that $\alpha_s + \alpha_f = 1$. Here α_s and α_f are the concentrations of solid and fluid phases by volume respectively. The laws of conservation of mass (continuity equation) and momentum equation are satisfied by each phase individually which are coupled through pressure and inter-phasial exchange

coefficients.

The forces acting on a single particle in the slurry:

1. Static pressure gradient, ∇P.
2. Solid pressure gradient or the inertial force due to particle interactions, ∇Ps
3. Drag force caused by the velocity difference between two phases, $K_{sf}\left(\vec{v}_s - \vec{v}_f\right)$ where K_{sf} is the inter-phase drag coefficient and $\overrightarrow{v_s}$ & $\overrightarrow{v_f}$ are velocity of solid and fluid phase respectively.
4. Viscous forces, $\nabla.\overline{\overline{\tau}}_f$ where $\overline{\overline{\tau}}_f$ is the stress tensor for fluid.
5. Body forces, $\rho\vec{g}$, where, ρ is the density and g is acceleration due to gravity.
6. Virtual mass force, $C_{vm}\alpha_s\rho_f\left(\overrightarrow{v_f}.\nabla\overrightarrow{v_f} - \overrightarrow{v_s}.\nabla\overrightarrow{v_s}\right)$ where C_{vm} is the coefficient of virtual mass force and is taken as 0.5 in the present study.
7. Lift force, $C_L\alpha_s\rho_f\left(\overrightarrow{v_s} - \overrightarrow{v_f}\right)\times\left(\nabla\times\overrightarrow{v_f}\right)$ where C_L is the lift coefficient taken as 0.5.

III NUMERICAL SOLUTION

3.1. Geometry Generation

The computational grids for 3.8 m long, 54.9 mm internal diameter horizontal pipe is generated using GAMBIT 2.4.6 and is having 2,40,236 hexahedral volume cells (Figure 1) finalized conducting proper mesh independency check. The length of pipe is sufficiently long (i.e., more than 50*D*, where *D* is the pipe diameter) for fully developed flow. The presence of fully developed flow is confirmed by studying the computational results for pressure drop along the slurry pipeline which attains a constant value after a distance of 0.5 m from the inlet; indicating the onset of fully developed flow. The computed pressure drops presented in the present study are those calculated in the last one metre of the pipeline, whereas concentration and velocity distributions are observed at the outlet.

In order to capture the steep gradients of flow parameters near the walls, a boundary layer mesh containing four layers within a distance of 5% of the diameter of the pipe, has been generated. It helps in improving the performance of the wall function and also to fulfill the requirement of y^+ = 30 near the wall, required for better convergence. Here, y^+ is the dimensionless wall distance for the cell adjacent to the wall. Meshing in rest of the flow domain is done using the hexagonal shape and Cooper type element, which uses an algorithm to sweep the mesh node patterns of specified "source" faces through the volume.

3.2. Boundary conditions

The flow domain under consideration is having three boundaries: the inlet boundary, the outlet boundary and the wall boundary. Velocity and volume fraction of liquid and solid phases have been mentioned at the inlet cross-

section of the pipe, i.e., $Vm = v_s = v_f$, $\alpha_s = C_{vf}$ and $\alpha_f = (1- C_{vf})$. Here, V_m is the mean flow velocity which was measured experimentally using electromagnetic flow meter. And, C_{vf} is the efflux concentration in the slurry pipe and can be expressed as:

$$C_{vf} = \frac{1}{A}\int_A \bar{\alpha}_s dA \cong \frac{1}{A}\int_A \alpha_s dA \qquad \text{Eq. 1}$$

At walls, no slip condition has been adopted for liquid phase whereas for solid phase specularity co-efficient of 0.99 has been specified to account for pipe roughness.

3.3. Solution strategy and convergence criteria

Commercial CFD software 'FLUENT 6.3.26' based on finite volume method has been used for simulation of slurry flow with boundary conditions and turbulence model described in previous sections. A convergence criterion 10^{-3} has been adopted with second order upwind discretization for momentum equation and first order upwind discretization for volume fraction, turbulent kinetic and turbulent dissipation energy. These schemes help in ensuring satisfactory accuracy, stability and convergence.

IV MODELING RESULTS

4.1 Concentration distribution

Eulerian model results for concentration distribution have been plotted in Figs. 1-6 at different C_{vf} and V_m. From these figures, it is observed that particles are dispersing in such a way that their interaction with pipe wall is increasing with increase in flow velocity. Further, it is observed that variation of solids concentration in the horizontal plane becomes more noticeable as the C_{vf} and flow velocity increases. For most of the data, the higher concentration zone, is situated in the lower half portion at the bottom of pipe, which is due to the gravitational effect. However, at higher C_{vf} and flow velocities, the higher concentration zones are situated in the lower half portion of pipeline away from the surrounding pipe wall.

4.2 Velocity distribution

Figs. 7-12 show the velocity distributions $\upsilon_{sy}(x,z)$ at C_{vf} of 5, 10, 20, 30, 40 and 50%, respectively. $\upsilon_{sy}(x,z)$ is the *y*-component of solid velocity perpendicular to the pipe cross-section (*x*-*z* plane). It is observed that at lower C_{vf} and $V_{m,}$ the solids velocity distribution is asymmetric having relatively smaller velocities in the lower half of the pipe due to larger shear force. However, the velocity distributions tend to become symmetric as the velocity and concentration increase. The reason for obtaining symmetric velocity distributions may be attributed to the increased turbulence resulting into the complete mixing of fluid and solid particles at higher C_{vf} and V_m.

V CONCLUSION

The Eulerian two-phase model of FLUENT was found to aptly capture the flow behavior of slurry transport through pipeline. It clearly identified the intriguing features in flow domain which enabled one to reasonably explain the flow behavior of slurry through pipeline.

REFERENCES

1. Ismail, H.M. (1952). Turbulent transfer mechanism and suspended sediment in closed channels. *Trans. ASCE*, 117, 409-446.
2. Jiang, Y. Y., & Zhang, P. (2012). Numerical investigation of slush nitrogen flow in a horizontal pipe. *Chemical Engineering Science*, *73*, 169-180.
3. Kaushal, D.R., Sato K., Toyota T., Funatsu K. and Tomita Y. (2005). Effect of particle size distribution on pressure drop and concentration profile in pipeline flow of highly concentrated slurry. *International Journal of Multiphase Flow*, 31, 809-823.
4. Kumar, N., Gopaliya, M.K. and Kaushal, D.R. (2016). Modeling for slurry pipeline flow having coarse particles. *Multiphase Science and Technology*, An International Journal, Vol. 28, Issue 1, pp 1-33.
5. Kumar, N., Gopaliya, M.K. and Kaushal, D.R. (2017). Experimental investigations and CFD modeling for flow of highly concentrated iron ore slurry through horizontal pipeline. *Particulate Science and Technology*, An International Journal, Taylor and Francis Publications. (DOI: 10.1080/02726351.2017.1364313)
6. Krampa-Morlu, F.N., Bergstrom, D.J., Bugg, J.D., Sanders, R.S., Schaan and J. (2004). Numerical simulation of dense coarse particle slurry flows in a vertical pipe. *Proceedings of the Fifth International Conference on Multiphase Flow*, ICMF'04, Paper No. 460.
7. Lin, C. X. and Ebadian, M.A. (2007). A numerical study of developing slurry flow in the entrance region of a horizontal pipe. *Journal of Computer & Fluids*, 37, 965-974.
8. Ling, J., Skudarnov, P.V., Lin, C.X. and Ebadian, M.A. (2003). Numerical investigations of liquid solid slurry flows in a fully developed turbulent flow region. *International Journal of Heat and Fluid Flow*, 24, 389-398.
9. O'Brien, M.P. (1933). Review of the theory of turbulent flow and its relations to sediment transportation. *Trans. Am. Geophys. Union*, 14, 487-491.
10. Rouse, H. (1937). Modern conceptions of the mechanics of fluid turbulence. *Trans. ASCE*, 102, 463-505.

ISBN: 978-93-86171-85-6

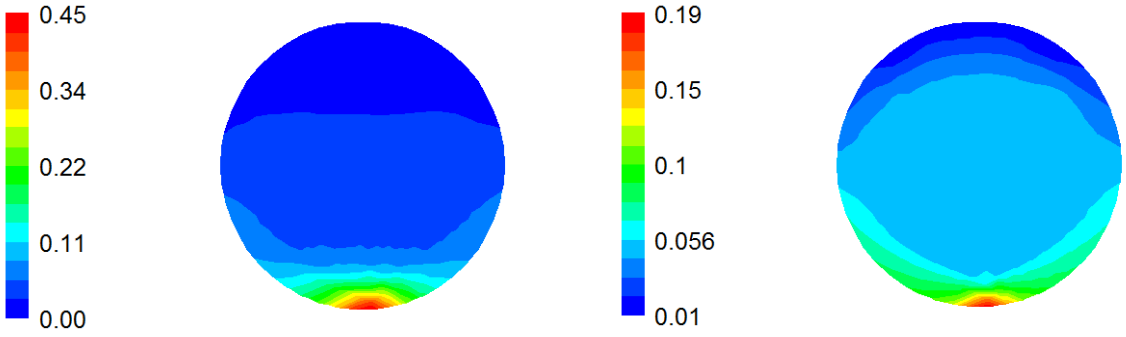

(a) V_m = 1 m/s (b) V_m = 2 m/s

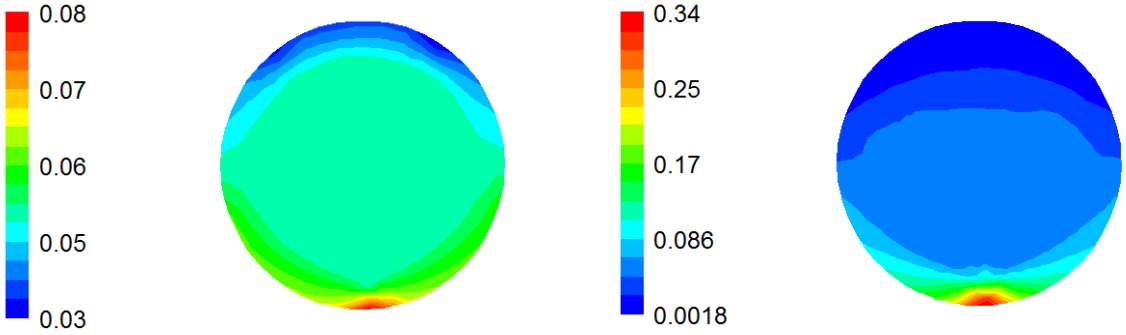

(c) V_m = 3 m/s (d) V_m = 4 m/s

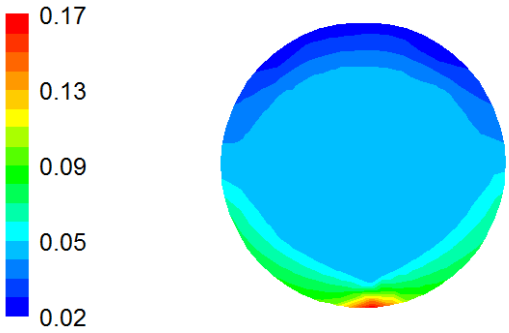

(e) V_m = 5 m/s

Fig. 1 Solid concentration profile α_s predicted by CFD at C_{vf} = 5%

ISBN: 978-93-86171-85-6

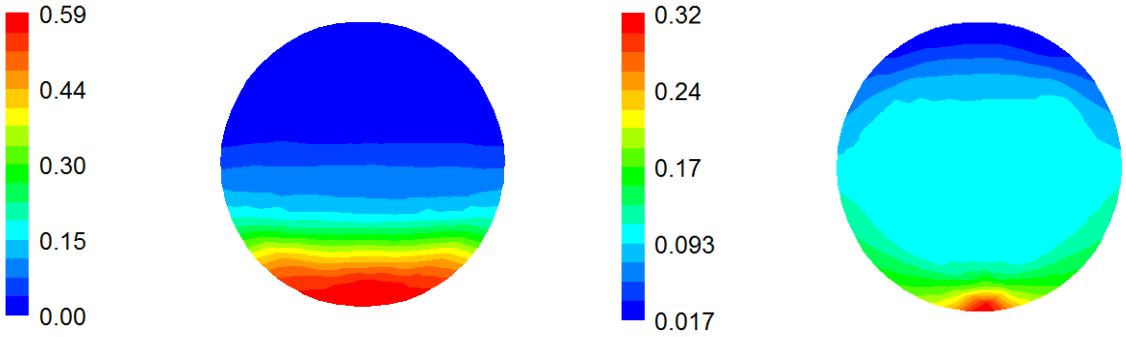

(a) V_m = 1 m/s (b) V_m = 2 m/s

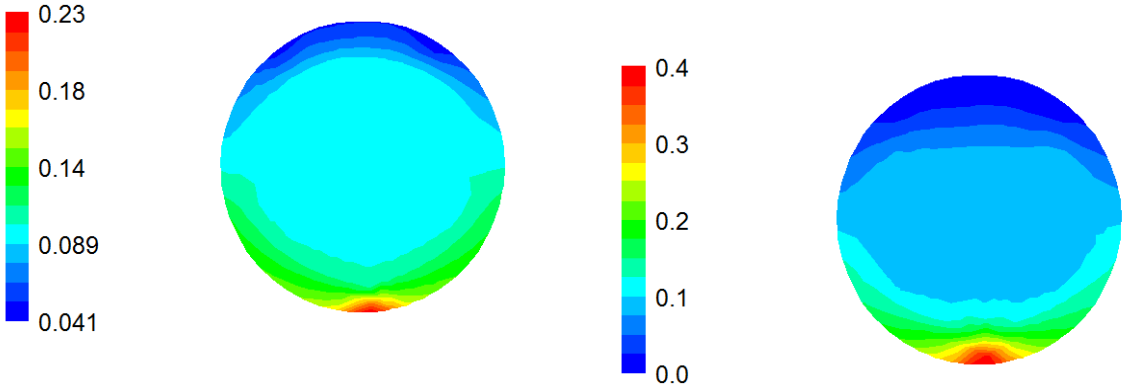

(c) V_m = 3 m/s (d) V_m = 4 m/s

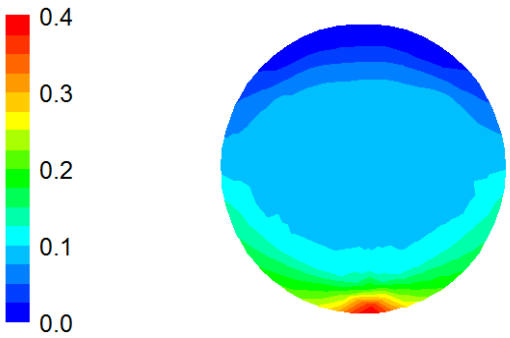

(e) V_m = 5 m/s

Fig. 2 Solid concentration profile α_s predicted by CFD at C_{vf} = 10%

ISBN: 978-93-86171-85-6

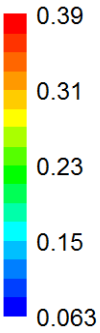

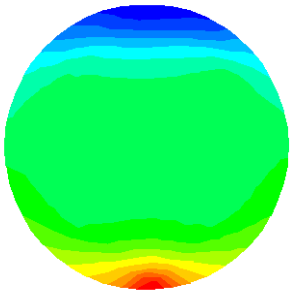

(a) V_m = 1 m/s

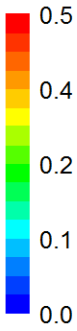

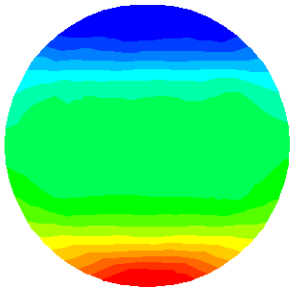

(b) V_m = 2 m/s

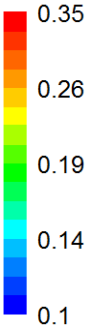

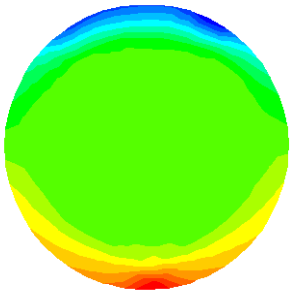

(c) V_m = 3 m/s

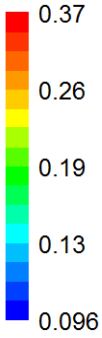

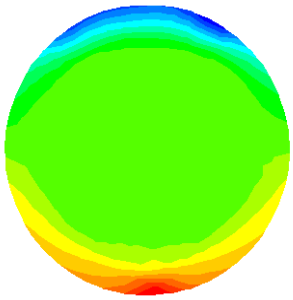

(d) V_m = 4 m/s

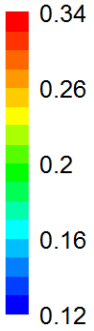

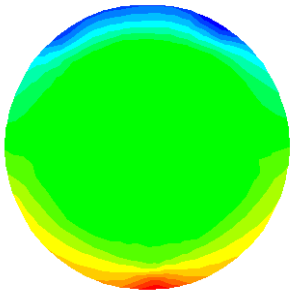

(e) V_m = 5 m/s

Fig. 3 Solid concentration profile α_s predicted by CFD at C_{vf} = 20%

ISBN: 978-93-86171-85-6

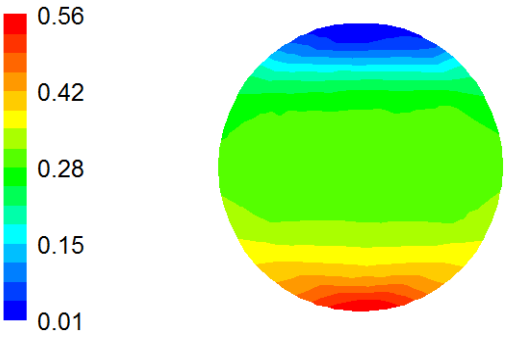

(a) V_m = 1 m/s

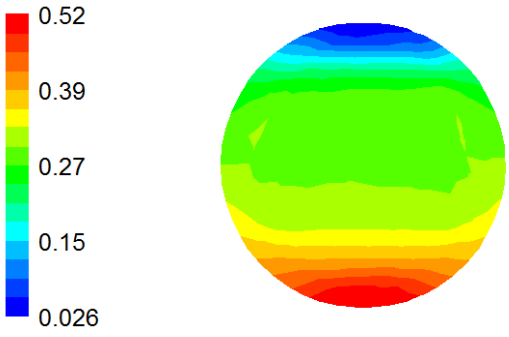

(b) V_m = 2 m/s

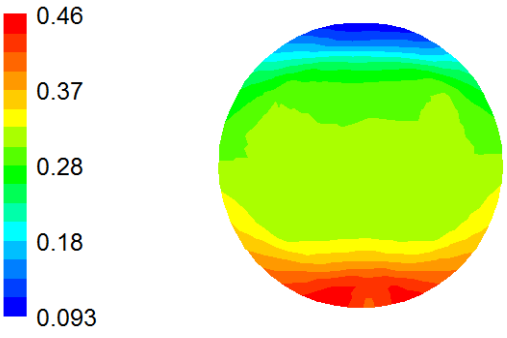

(c) V_m = 3 m/s

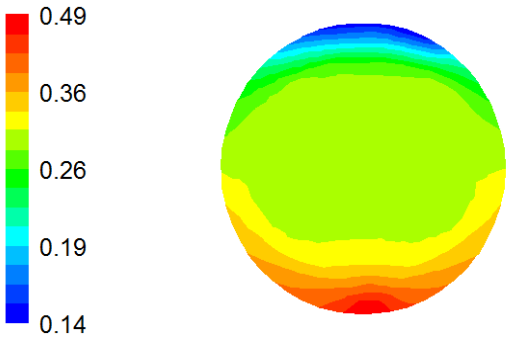

(d) V_m = 4 m/s

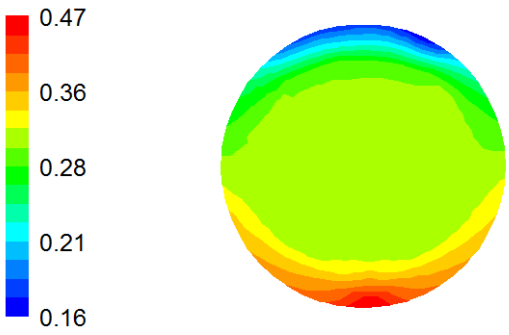

(e) V_m = 5 m/s

Fig. 4 Solid concentration profile α_s predicted by CFD at C_{vf} = 30%

ISBN: 978-93-86171-85-6

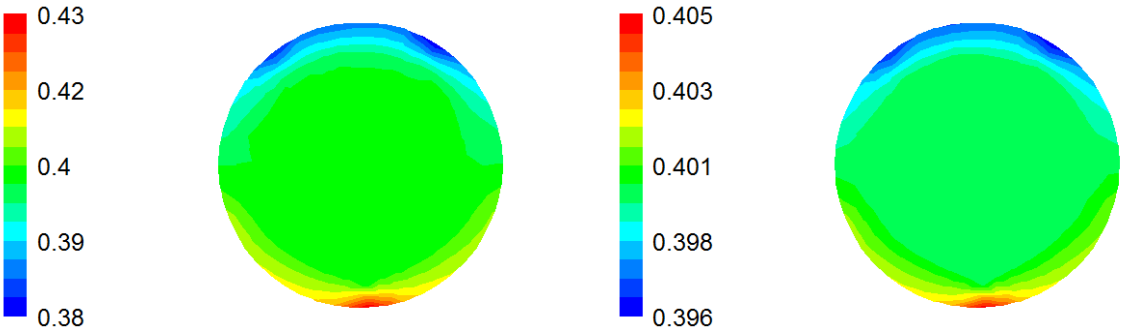

(a) V_m = 2 m/s (b) V_m = 3 m/s

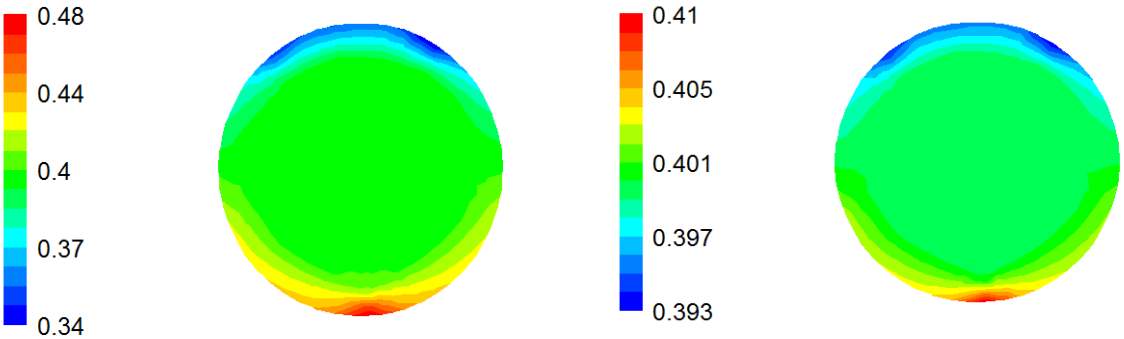

(c) V_m = 4 m/s (d) V_m = 5 m/s

Fig. 5 Solid concentration profile α_s predicted by CFD at C_{vf} = 40%

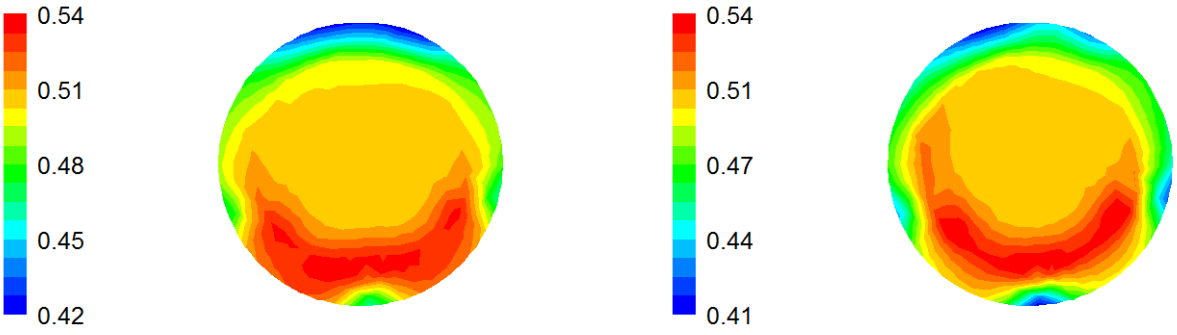

(a) V_m = 3 m/s (b) V_m = 4 m/s

Fig. 6 Solid concentration profile α_s predicted by CFD at C_{vf} = 50%

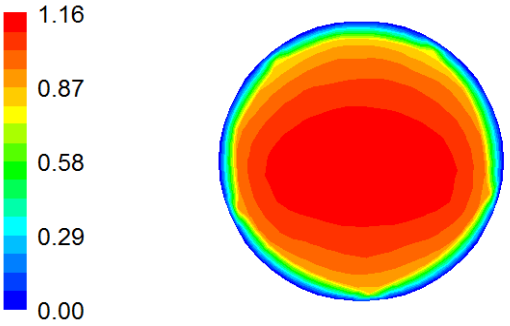

(a) V_m = 1 m/s

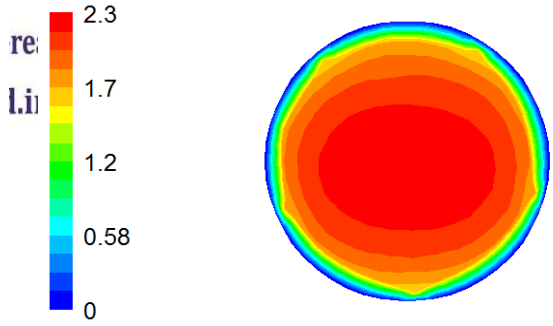

(b) V_m = 2 m/s

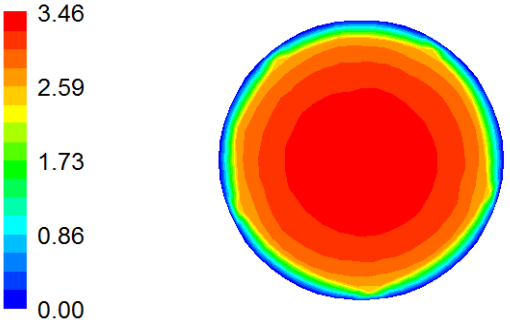

(c) V_m = 3 m/s

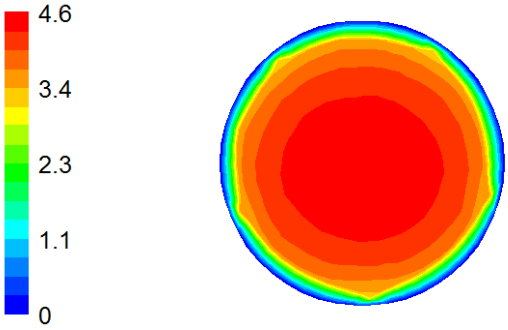

(d) V_m = 4 m/s

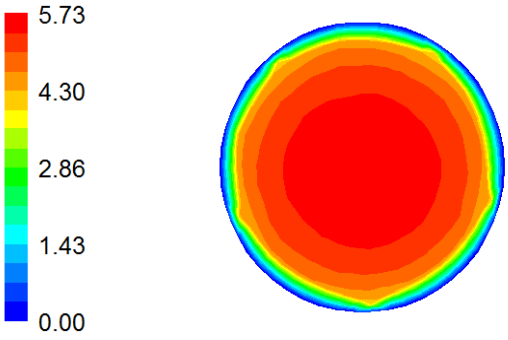

(e) V_m = 5 m/s

Fig. 7 Velocity profile $\upsilon_{sy}(x,z)$ in m/s predicted by CFD at C_{vf} = 5%

ISBN: 978-93-86171-85-6

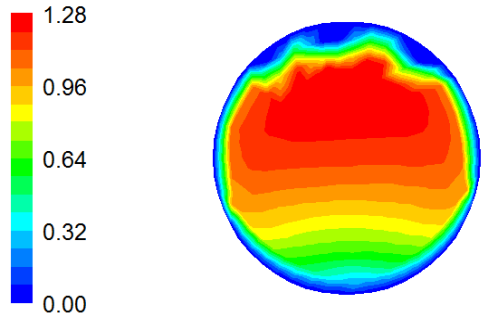

(a) V_m = 1 m/s

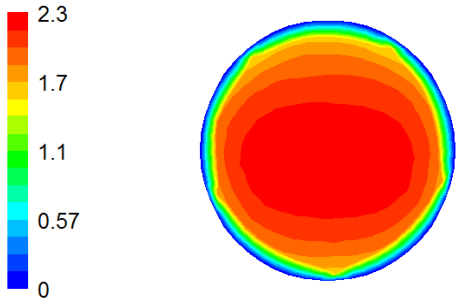

(b) V_m = 2 m/s

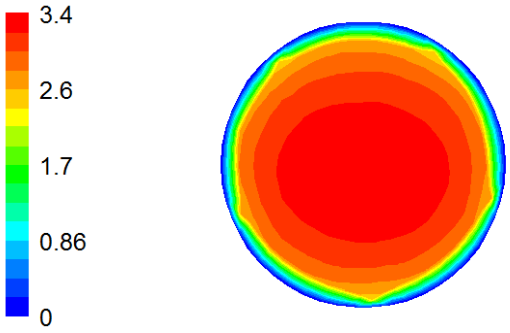

(c) V_m = 3 m/s

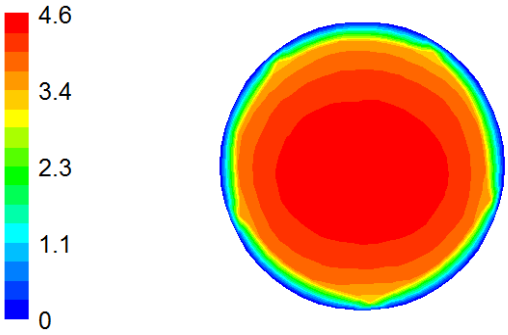

(d) V_m = 4 m/s

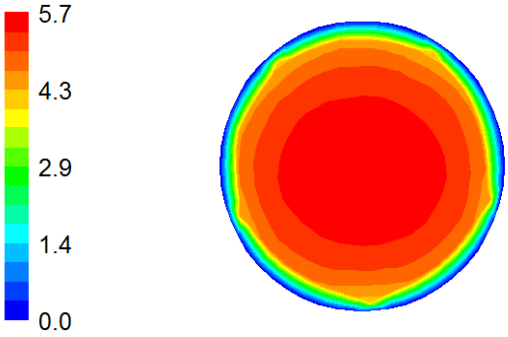

(e) V_m = 5 m/s

Fig. 8 Velocity profile $\upsilon_{sy}(x,z)$ in m/s predicted by CFD at C_{vf} = 10%

ISBN: 978-93-86171-85-6

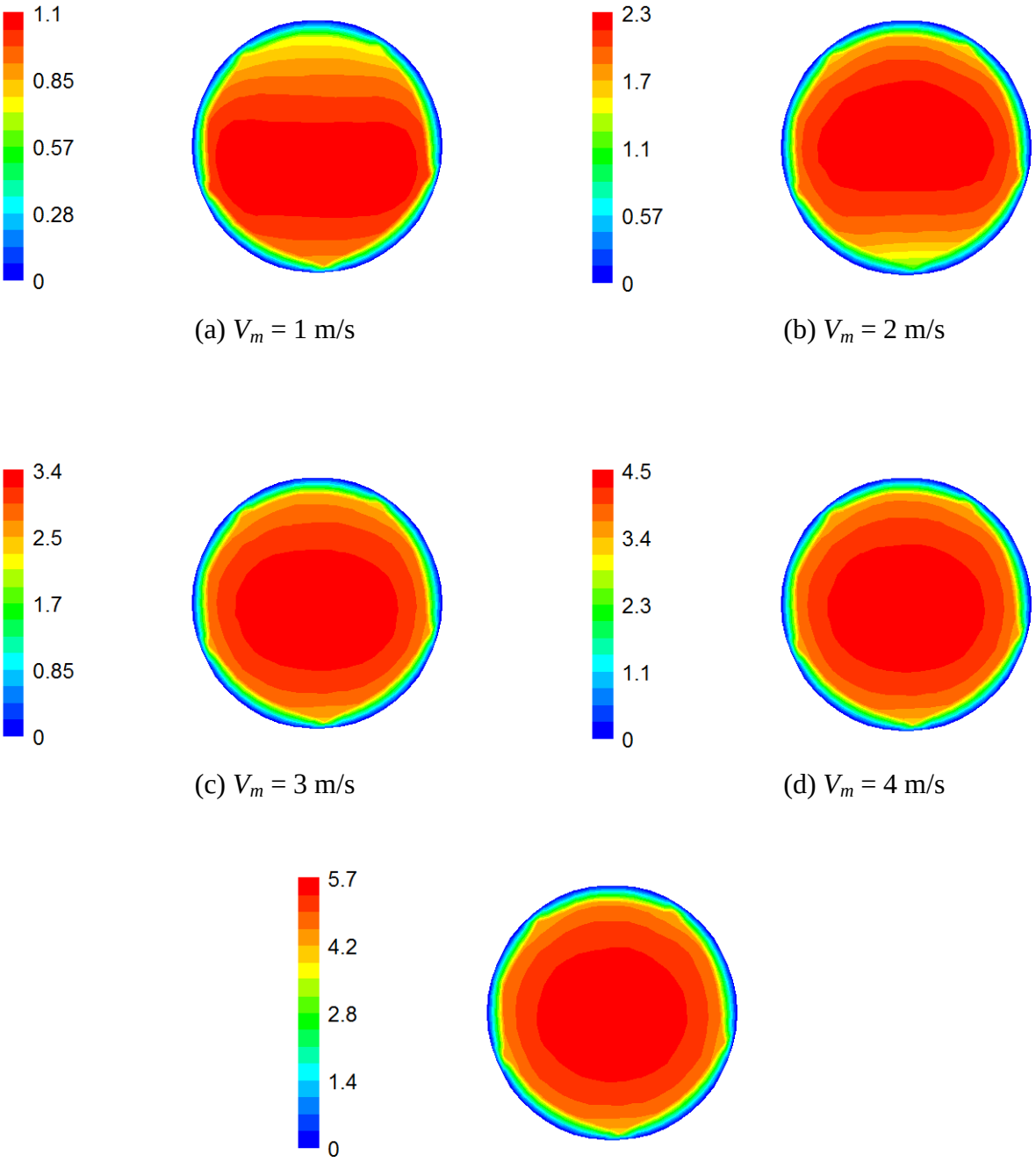

(a) V_m = 1 m/s

(b) V_m = 2 m/s

(c) V_m = 3 m/s

(d) V_m = 4 m/s

(e) V_m = 5 m/s

Fig. 9 Velocity profile $\upsilon_{sy}(x,z)$ in m/s predicted by CFD at C_{vf} = 20%

ISBN: 978-93-86171-85-6

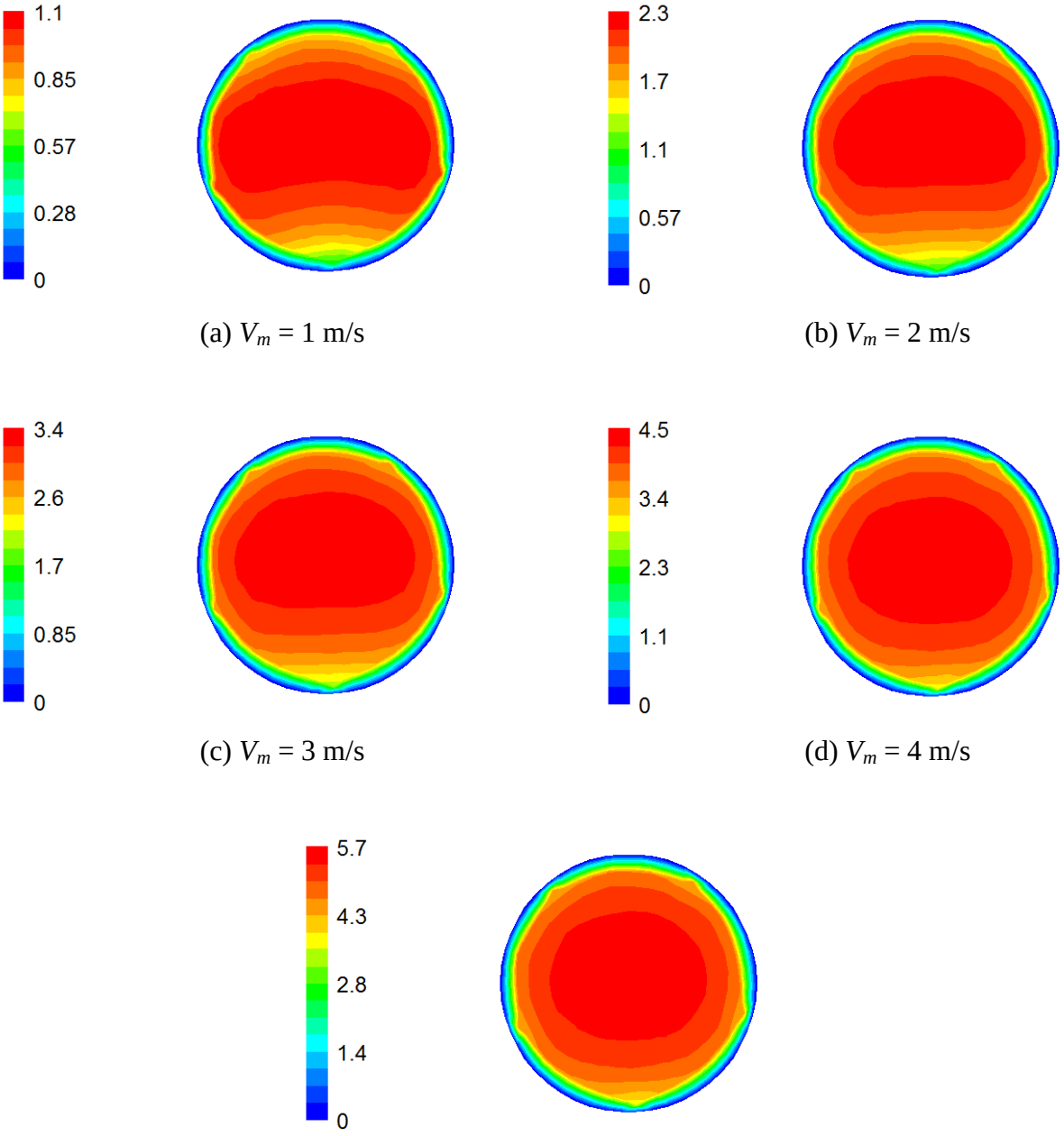

(a) V_m = 1 m/s

(b) V_m = 2 m/s

(c) V_m = 3 m/s

(d) V_m = 4 m/s

(e) V_m = 5 m/s

Fig. 10 Velocity profile $\upsilon_{sy}(x,z)$ in m/s predicted by CFD at C_{vf} = 30%

 ISBN: 978-93-86171-85-6

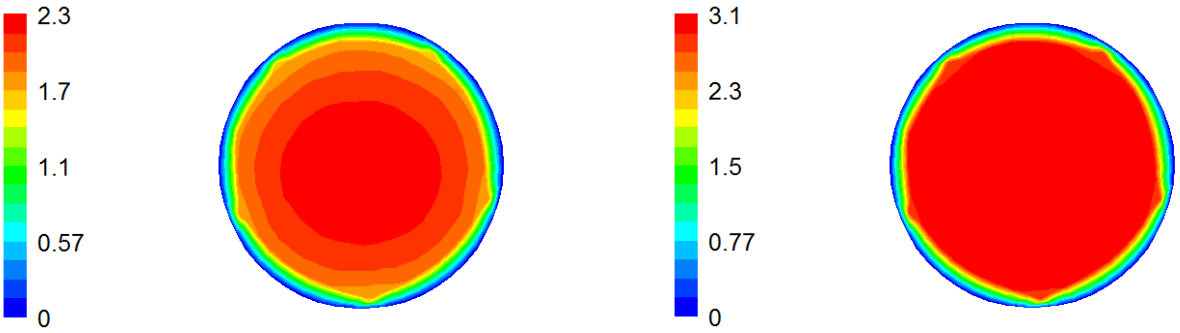

(a) V_m = 2 m/s (b) V_m = 3 m/s

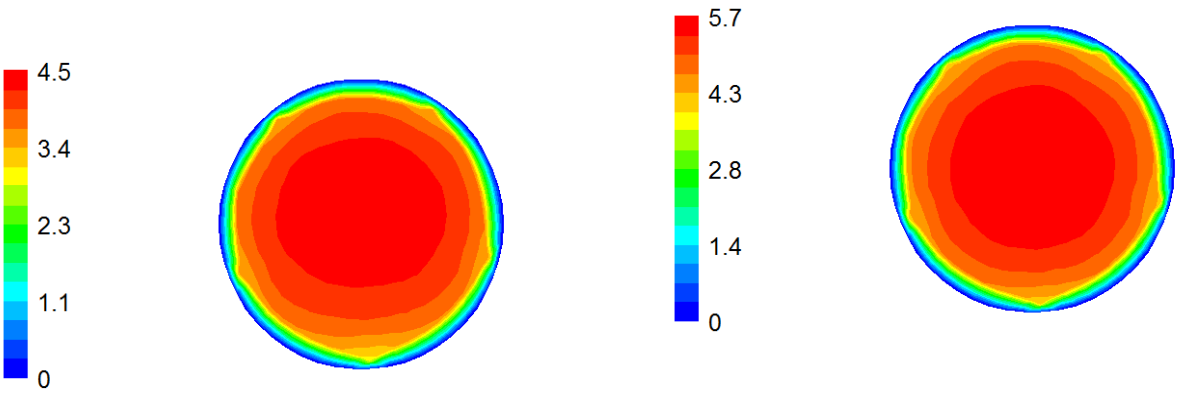

(c) V_m = 4 m/s (d) V_m = 5 m/s

Fig. 11 Velocity profile $\upsilon_{sy}(x,z)$ in m/s predicted by CFD at C_{vf} = 40%

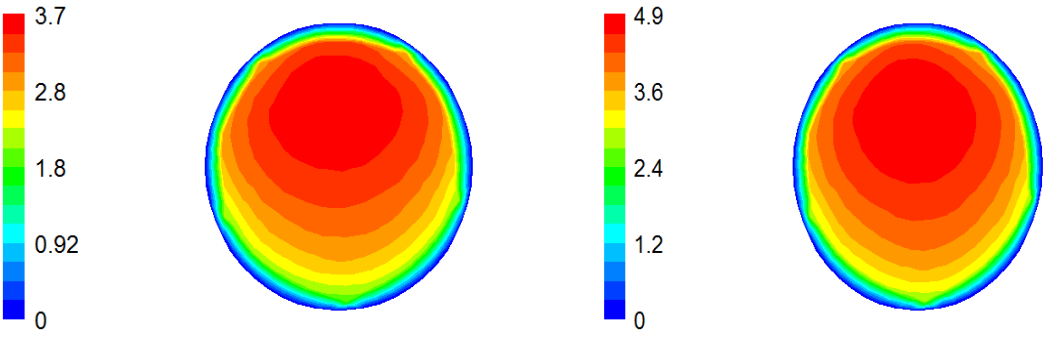

(a) V_m = 3 m/s (b) V_m = 4 m/s

Fig. 12 Velocity profile $\upsilon_{sy}(x,z)$ in m/s predicted by CFD at C_{vf} = 50%